Evaluate the Feasibility of Gd-based Contrast Clearance Differenceto Delineate Subvolume Target in Primary and Metastatic Brain Tumors Radiotherapy- A Prospective Study

Yin Xing Wang
Shandong Cancer Hospital and Institute, Shandong First Medical University and Shandong Academy of Medical Sciences https://orcid.org/0000-0003-3689-6198

Guan Zhong Gong
Shandong Cancer Hospital and Institute, Shandong First Medical University and Shandong Academy of Medical Sciences

Ya SU
Shandong Cancer Hospital and Institute,Shandong First Medical University and Shandong Academy of Medical Sciences

Li Zhen WANG
Shandong Cancer Hospital and Institute,Shandong First Medical University and Shandong Academy of Medical Sciencess

Jie LU
Shandong Tumor Hospital and Institute, Shandong First Medical University and Shandong Academy of Medical Sciences

Yong Yin (yinyongsd@126.com)

Research

Keywords: Brain neoplasms, Sub-volume, Magneticresonanceimaging, Delayed contrast extravasation MRI

Posted Date: June 19th, 2020

DOI: https://doi.org/10.21203/rs.3.rs-36403/v1

Abstract

Background: To evaluate the feasibility ofdelineating subvolume target in brain tumor radiotherapy using gd-based contrast clearance difference.

Methods：Twenty-six patients with malignant brain tumor were scanned with MRI. The first and second acquisitions of standard T2-weighted images (T2WI) andT1-weighted images (T1WI) were respectively performed?> at 5 minutes and 60 minutesafter injection of contrast agent. Delayed contrast extravasation MRI(DCEM) computed by Brainlab concludesregions of contrast agent clearance which represent active tumor，andregions of contrast accumulation which represent non-tumor tissues. Based on T2WI images,14 patients were divided into group A and group B, with andwithout liquefaction necrosis, respectively. Then,gross target volume (GTV) was delineated on T1WI images. Based on the GTV, active tumor (GTV_{tumor}) and non-tumorregions($GTV_{non\text{-}tumor}$) were delineated on T1WI-DCEM fusion images, whileliquefaction necrosis ($GTV_{liquefaction}$)and non-liquefaction($GTV_{non\text{-}liquefaction}$)were delineated on T1-T2WI fusion images. Finally, the differences between different subvolumes were compared by paired t-test.

Results：In group A,the mean value of GTV_A was 21.38±25.70 cm^3, and the $GTV_{non\text{-}liquefaction}$ and $GTV_{liquefaction}$ were 13.65±18.15cm^3 and6.30±7.57cm^3, respectively. The GTV_{tumor} was 10.40±13.52 cm^3 whilethe $GTV_{non\text{-}tumor}$ was 9.55±14.57 cm^3, The $GTV_{non\text{-}liquefaction}$ increased by an average of 28.2%（P＜0.05）,compared to GTV_{tumor} . While the $GTV_{non\text{-}tumor}$ increased by an average of 46.3% (P＜0.05), compared tothe $GTV_{liquefaction}$.In group B, the mean value of GTV_B on enhanced T1WI was4.39±3.75 cm^3. The $GTV_{non\text{-}tumor}$reduced by an average of 50.3% (P＜0.05) , compared totheGTV $_{tumor}$.

Conclusion：Comparedto T2WI, the DCEM has advantages in identifyingthe liquefaction areaand could clearly differentiatesubvolume of active tumor from non-liquefaction necrosis.DCEMis meaningful in guiding the delineation of subvolume in primary and metastatic brain tumors.

Background

Radiotherapy is one of the indispensable treatment methods for brain tumor, whose effect is one of the significant factors affecting the survival of patients. With the development of radiotherapy technology, radiotherapy for brain tumors has achieved encouraging results. Magnetic resonance has become a routine method in the radiotherapy management of brain tumor patients by virtue of its high resolution of soft tissue [1–3]. At present, it is crucial to accurately identify tumor tissues from non-tumor tissues for individualized treatment of brain tumor patients, but traditional MR cannot distinguish the effects of tumor progression and treatment induction. Multimodal magnetic resonance imaging, such as MRS、PWI,could provide clinician with information which concluded tumor metabolism, pathophysiology, microcirculation state[4–5]. Combining the multimodal magnetic resonance imaging made the application of MR technique become more and more widely in detecting focus, guiding the tumor target

outline and observing therapeutic response dynamically. However, radiotherapy failure still occured from time to time, which may be related to the different sensitivity in multimodal magnetic resonance imaging and insufficient local Radiotherapy dose of tumors. In the era of precise radiotherapy, it was a research hotspot that identifying the biological characteristics of tumors in different regions before radiotherapy to achieve the intensity modulated radiotherapy within the tumor. PET was relatively insensitive to brain tumors, expensive and radioactive, which limited its wide application. so we may achieve biological IMRT(BIMRT) by applying MR to observe brain tumor characteristics. Leor et al. [6] showed that gd-based contrast clearance difference could provide reliable tumor load information and own potential value in predicting brain tumor recurrence. Therefore, we carried out a study that applyed gd-based contrast clearance difference on to delineate subvolume brain tumor and provided a basis for the design of future radiotherapy plans.

Methods

Patients

The study include 26 patients (mean age: 57 ± 12 years old) with brain tumor, 25 cases of patients with metastatic tumors, a case of patient with primary tumor, 14 men and 12 women, 37 tumor lesions. None of the patients received surgical resection in tumor area. Every tumor exceeded 0.5 cm^3.The study was approved by the Institutional Ethics Committee of Shandong Cancer Hospital and Institute, and written informed consent was obtained from all patients.

Mri Experiments

All MRI experiments were performed at 3T MR system (Discovery 750w, GE Healthcare, USA) with brain coil. For the T1WI measurement, the scan parameters were applied as follows: TR = 8.47 ms, TE = 3.25 ms, matrix = 256 × 256, FOV = 256 mm x256mm, slice thickness = 1 mm. For the T2WI measurement, the scan parameters were applied as follows: TR = 13312 ms, TE = 113.5/EF, FOV:26 × 26, slice thickness = 3 mm. A standard single dose (0.1 mmol/kg) of gadolinium DOTA was injected intravenously. MR sequences included T2 PROPELLER, T2 FLAIR and echo-planar diffusion-weighted MRI (DWI). The first acquisitions of standard T1-weighted images (T1WI) and T2-weighted images (T2WI) were performed at 5 minutes after injection of contrast agent while the second acquisitions of T1WI were performed at 60 minutes after injection of contrast agent.

DCEM acquisition

All images were uploaded to Brainlab software whose contrast clearance analysis module was performed by subtracting T1WI acquired 60 minutes after Gadolinium(Gd)-based contrast agent injection from those acquired 5 minutes post-Gd. Delayed contrast extravasation MRI(DCEM) computed by Brainlab concludes regions of contrast agent clearance which represent active tumor,and regions of contrast

accumulation which represent non-tumor tissues. The regions of active tumor were coded in blue while the regions were coded in other color.

Image processing

Based on different signal changes on T2WI images, patients were divided into group A which own T2WI high signal and group B, with and without liquefaction necrosis, respectively. DCEM were registrated rigidiy with the first T1WI enhanced image and T2WI in fusion module of Brainlab. In order to achieve accurate registration, the researchers can carry out manual adjustment or fine-tuning.

Then, gross target volume (GTV) was delineated on first T1WI images. Based on the GTV, active tumor (GTV_{tumor}) and non-tumor regions ($GTV_{non-tumor}$) were delineated on T1WI-DCEM fusion images, while liquefaction necrosis ($GTV_{liquefaction}$) and non-liquefaction ($GTV_{non-liquefaction}$) were delineated on T1-T2WI fusion images. All the target were delineated by the same researcher in Smartbrush module of Brainlab software. The volume of each target area was automatically generated by the software. Finally, the volume and statistical differences of different subvolume were calculated (Fig. 1).

Statistics

Data were analyzed using SPSS25.0 and represented mean ± standard deviation. Paired t-tests was used to determine the difference of sub-volume between DCEM and T2WI. Significance threshold was set as $p < 0.05$.

Results

Group **informations**

The mean value of GTV_{total} with 26 patients was (10.28 ± 17.25) cm^3. The mean value of GTV_A was (19.95 ± 25.26)cm^3 in group A where conclude 14 patients and 14 lesions. The mean value of GTV_B was 4.39 ± 3.75cm^3 where conclude 12 patients and 23 lesions (Tables 1 and 2). The GTV_A increased by an average of 15.56 cm^3, compared to GTV_B. DCEM could be divided into the following three types: Diffuse type, Marginal type and Mixed type, according to distribution characteristics of active tumor areas (Fig. 2) .DCEM of 37 lesions concluded 6 case of diffuse type whose pathological types were all adenocarcinoma, 9 case of Mixed type and 22 case of Marginal type.

Subvolume Target Informations

In group A, the non-liquefaction and liquefaction necrosis on T2WI were 13.65 ± 18.15 cm^3 and6.30 ± 7.57 cm^3, respectively. Active tumor area was 10.40 ± 13.52 cm^3 while the non-tumor area was 9.55 ± 14.57 cm^3, The non-liquefaction necrosis volume increased by an average of 28.2%(P0.05 ; Table 3 and

Fig. 2), compared to active tumor area. It suggested that the solid component region of T2WI was not completely the region with tumor activity. While the non-tumor tissues increased by an average of 46.3% (P□0.05), compared to the liquefactive necrosis tissues. It showed that DCEM could find the potential area of liquefactive necrosis which T2WI couldn't display (Fig. 3).

In group B, the mean value of GTV_B on enhanced T1WI was 4.39 ± 3.75 cm^3. The $GTV_{non-tumor}$ reduced by an average of 50.3% (P□0.05 Table 4), compared to the GTV_{tumor}. It found that The detection of small brain tumors by DCEM still revealed tiny potential areas of liquefactive necrosis which T2WI couldn't detect.

Table 1
The volume and proportion of each target area(Mean±SD)

Group	Subvolume	Volume(cm^3)	Volume ratio(%)
Total	GTV_{Total}	10.28 ± 17.25	—
A	GTV_A	19.95 ± 25.26	—
	GTV_{tumor}	10.40 ± 13.52	52.9 ± 18.5
	$GTV_{non-tumor}$	9.55 ± 14.57	47.1 ± 18.5
	$GTV_{liquefaction}$	6.30 ± 7.57	32.2 ± 15.3
	$GTV_{non-liquefaction}$	13.65 ± 18.15	67.8 ± 15.3
B	GTV_B	4.39 ± 3.75	—
	GTV_{tumor}	3.02 ± 2.78	66.8 ± 18.7
	$GTV_{non-tumor}$	1.37 ± 1.42	33.2 ± 18.7

Table 2
The tumor information of 26 patients

Patient	Tumor	T2WI	Tumor type
1	1	liquefaction	Lung cancer with brain metastasis
2	1	liquefaction	Lung cancer with brain metastasis
3	1	liquefaction	Lung cancer with brain metastasis
4	1	liquefaction	Lung cancer with brain metastasis
5	1	Liquefaction	GBM
	2	Non- liquefaction	
6	1	Liquefaction	Colorectal cancer with brain metastasis
7	1	Liquefaction	Lung cancer with brain metastasis
	2	Non- liquefaction	
	3	Non- liquefaction	
8	1	Liquefaction	Lung cancer with brain metastasis
9	1	Liquefaction	breast cancer with brain metastasis
10	1	Liquefaction	Lung cancer with brain metastasis
11	1	Liquefaction	Lung cancer with brain metastasis
12	1	Liquefaction	Endometrial cancer with brain metastasis
13	1	Liquefaction	Lung cancer with brain metastasis
		Non- liquefaction	
14	1	Liquefaction	Lung cancer with brain metastasis
	2	Non- liquefaction	
15	1	Non- liquefaction	Renal carcinoma with brain metastasis
16	1	Non- liquefaction	Lung cancer with brain metastasis
17	1	Non- liquefaction	Lung cancer with brain metastasis
	2		
	3		
18	1	Non- liquefaction	Lung cancer with brain metastasis

Patient	Tumor	T2WI	Tumor type
19	1	Non- liquefaction	Lung cancer with brain metastasis
	2		
	3		
20	1	Non- liquefaction	Lung cancer with brain metastasis
21	1	Non- liquefaction	Esophagus cancer with brain metastasis
	2		
22	1	Non- liquefaction	biliary duct cancer with brain metastasis
	2		
23	1	Non- liquefaction	Lung cancer with brain metastasis
24	1	Non- liquefaction	cardial carcinoma with brain metastasis
25	1	Non- liquefaction	Lung cancer with brain metastasis
26	1	Non- liquefaction	Lung cancer with brain metastasis

Table 3
Subvolume information in Group A

Patient	GTV (cm^3)	GTV_{tumor} (cm^3) GTV_{tumor}/ GTV (%)	$GTV_{non-tumor}$ (cm^3) $GTV_{non-tumor}$/GTV (%)	$GTV_{liquefaction}$ (cm^3) $GTV_{liquefaction}$/GTV (%)	$GTV_{non-liquefaction}$ (cm^3) $GTV_{non-liquefaction}$/ GTV (%)
1	9.54	7.46 78.2	2.08 21.8	0.47 4.9	9.07 95.1
2	1.12	0.54 48.2	0.58 51.8	0.39 34.8	0.73 65.2
3	0.90	0.11 12.2	0.79 87.8	0.49 54.4	0.41 45.6
4	2.49	1.74 69.9	0.75 30.1	0.54 21.7	1.95 78.3
5	17.10	11.50 67.3	5.60 32.7	3.05 17.8	14.05 82.2
6	11.00	4.05 36.8	6.95 63.2	3.29 29.9	7.71 70.1
7	13.00	5.81 44.7	7.19 55.3	6.12 47.1	6.88 52.9
8	36.90	19.50 52.8	17.40 47.2	12.20 33.1	24.70 66.9
9	22.30	12.20 54.7	10.01 45.3	13.00 58.3	9.30 41.7
10	69.90	50.00 71.5	19.90 28.5	19.00 27.2	50.90 72.9
11	2.27	1.06 46.7	1.21 53.3	0.62 27.3	1.65 72.7
12	79.30	23.9 30.1	55.40 69.9	23.00 29.0	56.30 71.0
13	12.10	6.74 55.7	5.36 44.3	5.86 48.4	6.24 51.6
14	1.40	1.01 72.1	0.39 27.9	0.23 16.4	1.17 83.6
Mean	19.95	10.40 52.9	9.55 47.0	6.30 32.2	13.65 67.8
SD	25.26	13.52 18.5	14.57 18.5	7.57 15.3	18.15 15.3

Table 4
subvolume information in Group B

Patient	GTV (cm^3)	GTV_{tumor} (cm^3)	GTV_{tumor}/ GTV (%)	$GTV_{non-tumor}$ (cm^3)	$GTV_{non-tumor}$/GTV (%)
1	10.80	9.48	87.8	1.32	12.2
2	0.70	0.26	37.1	0.44	62.9
3	3.88	2.52	64.9	1.36	35.1
4	1.36	1.14	83.8	0.22	16.2
5	1.44	0.79	54.9	0.65	45.1
6	13.10	8.57	65.4	4.53	34.6
7	7.23	5.86	81.1	1.37	18.9
8	2.16	1.86	86.1	0.30	13.9
9	4.25	3.05	71.8	1.20	28.2
10	2.36	1.83	77.5	0.53	22.5
11	3.05	2.23	73.1	0.82	26.7
12	2.54	1.56	61.4	0.98	38.6
13	4.78	4.48	93.7	0.30	6.3
14	1.62	1.36	84.0	0.26	16.0
15	6.23	3.98	63.9	2.25	36.1
16	0.92	0.71	77.2	0.21	22.8
17	8.80	7.39	84.0	1.41	16.0
18	6.12	2.10	34.3	4.02	65.7
19	2.24	0.77	34.4	1.47	65.6
20	12.40	7.09	57.2	5.31	42.8
21	2.44	0.70	28.7	1.74	71.3
22	0.76	0.46	60.5	0.30	39.5
23	1.81	1.33	73.5	0.48	26.5
Mean	4.39	3.02	66.8	1.37	33.2
SD	3.75	2.78	18.7	1.42	18.7

Discussion

Cerebral metastases and glioma were the most common and highest aggressive malignant tumor, that could be locally controlled by radiation therapy, so as to slow down the disease progression and prolong survival time of patients. Although intensity-modulated radiation therapy has reached uniform distribution of dose in tumor area, but Radiotherapy failure still exists, on account of homogeneous distribution of tumor cells[7] and differences in radiation sensitivity.

Hazle et al. [8] found that radioactive necrosis and tumor tissues were enhanced at different rates by scanning T1WI enhanced images after a delay of 10–15 minutes, and further identified the recurrent tumor and radioactive necrosis area by delayed scanning. Leor et al. [9] suggested that the longer you delayed, the easier you will find tumor tissue, respectively, comparing T1WI enhanced images of 30 patients with the delay of 15 minutes and 75 minutes with postoperative samples. There was no significant difference between primary and metastatic brain tumors. One or more of the following characteristics of tumor morphology were the tumor tissue activity criteria in DCEM: cellularity, small cells, mitosis, high Ki67, pseudo-palisading necrosis and vascular proliferation. The criteria for non-tumor activity were the following: large, widely spaced atypical astrocytes, blood vessels hyalinization, fibrinoid material in vessels, proliferating small vessels and non-palisading tumor necrosis. Since each patient needed two T1WI enhanced scanning, In order to avoid the discomfort of waiting for a long time on the MR machine, we asked the patients to leave the machine after the first MR scan and perform the second scan after resting for 1 hour, so as to improve the efficiency of the experiment. The operator positioning errors could reach more than 5□□, based on the subjective experience and fixed thermoplastic mask, while the allowable error of the positioning fixator is generally ± 2 mm in radiotherapy. In order to achieve sufficiently accurate degree in the experiment, we recruited 26 patients who have undergone CT simulation positioning. Same operators could reduce the involuntary movement and increase scanning repeatability by mask production that could be used to mark relative position between the mesh of mask and skin of forehead and quality control of every aspect.

Evaluation means of radiotherapy failure were relatively limited at present. Conventional MR has apparently not distinguished active area and high risk of recurrence from tumor area, especially In the case of complex situation that conclude fibroplasia and peritumoral edema. Weybright et al. [10, 11] found that Cho/Cr > 2 and (or) Cho/NAA > 2. 5 prompted tumor recurrence by means of studying metabolites of recurrent gliomas, but whose disadvantage was that not independent indicator for diagnosis. Functional MRI which concluded DSC-MRI and DCE-MRI could effectively evaluate vascular permeability and angiogenesis [12]. Some studies have shown that value of relative cerebral blood volume (rCBV) could be seen as one of the most valuable parameters for evaluating tumor classification [13]. Wang et al. [14] found that glioma had no recurrence according to rCBV < 1 by means of perfusion weighted imaging (PWI), while rCBV > 2 suggested greater possibility of recurrence, DSE based on PWI could assess tumor status and predict tumor behavior. ASL PWI based could predict blood vessel density, which was strongly correlated with tumor and more stable than DCEM [15, 16]. Leor et al. [6, 9] found that the regions where contrast agent clear rapidly in DCEM were significantly correlated with high rCBV.

However, enhanced lesions with high rCBV had no statistical difference comparing with regions of interest (ROI) which were the same shape and size on the opposite normal brain organization. It suggested that high CBV in opposite normal brain anatomy may hide the accuracy of functional magnetic resonance. The high rCBV in the tumor region was statistically different from the contralateral ROI when tumor location separated from gray matter. The mean blue volume of the enhanced tumor region on DCEM was statistically significantly different from contralateral ROI. It indicated that DCEM was less affected by the normal contralateral tissue. Leor et al. also found that DCEM, whose sensitivity was up to 90% in detecting active tumors, could clearly show the small lesions which were not detected by DSC-MRI and couldn't find artifacts which were prone to appear due to anatomical factors in DSC-MRI.

This study, based on distinguishing tumor activity from DCEM and liquefactive necrosis from T2WI, found that DCEM could find the potential areas of liquefactive necrosis which T2WI couldn't display. Tumor cells can't proliferate owe to reduction of blood supply which was due to Immature vessel, Clogged vascular lumen by endothelial cell and medical intervention such as radiotherapy, chemotherapy and so on. It bought about which tumor cells with earlier blood disruption slowly evolved into liquefaction necrosis. Liquefaction necrosis was high signal in T2WI, on account of high sensitivity to free water. However, tumor cells which were neither activation nor blood supply which disappeared later didn't become liquefaction. It made some part of $GTV_{non-tumor}$ be disappeared in T2WI. Based on this conclusion, DCEM could provide the trend or degree of tumor necrosis for clinicians. Of course, tumor cells without blood supply may become fibrosis. A patient with brain metastases from breast cancer existed in the phenomenon where $GTV_{liquefaction}$ (13 cm^3)were larger than $GTV_{non-tumor}$（10.1 cm^3）in group A. We thought that it is large volume of free water generated by large necrotic area that covered the part of active tumor area, so as to show the larger necrotic in T2WI.

According to the statistical data of group B, the average volume of tumor was smaller than group A. Although T2WI did not indicate liquefaction necrosis, but the $GTV_{non-tumor}$ could be detected on DCEM, on the one hand it further proved the advantage in finding potential necrosis area, on the other hand this advantage was also applicable to small brain tumors. This conclusion was similar to Leor's opinion that DCEM is more sensitive to MR in detecting small brain tumors. In group A, $GTV_{non-liquefaction}$ was larger than GTV_{tumor}, in other words, the active tumor area was not completely the solid tumor component on T2WI. Leor's study showed that the clearance differences of Gd-based contrast agents could reflect reliable tumor load information and had potential value in predicting brain tumor recurrence. Therefore, we considered that GTV_{tumor} had higher risk of recurrence than other solid tumor regions. It was hysteretic to predict the prone relapse areas of tumor in DCEM. It was more significant to control recurrence areas of high risk in advance. Therefore, we were able to delineate GTV_{tumor} before radiotherapy and to design a radiotherapy plan with a higher dose so as to improve local control of the tumor. Because according to Walker's report [17, 18], there was an obvious dose-response relationship that the survival rate of patients would improve with the increase of radiotherapy dose in tumor areas.

In clinical application, there was no doubt that it still existed in many problems, such as the improvement of image registration accuracy, the choice of dose in the high-risk area, the choice of tumor type and the progression tendency of non-tumor areas which were beyond the necrotic areas. In addition, In order to apply DCEM to clinical radiotherapy, we were supposed to evaluate it in all directions, combining with multidisciplinary and multi-image.

Conclusion

Compared to T2WI, the DCEM has advantages in identifying the liquefaction area and could clearly differentiate subvolume of active tumor from non-liquefaction necrosis. DCEM is meaningful in guiding the delineation of subvolume in primary and metastatic brain tumors.

Abbreviations

T2WI
T2-weighted images ;T1WI T1-weighted images DCEM Delayed contrast extravasation MRI GTV Gross Target Volume GTV $_{tumor}$ active tumor GTV $_{non-tumor}$ non-tumor regions GTV $_{non-liquefaction}$ non-liquefaction GTV $_{liquefaction}$ liquefaction necrosis BIMRT:biological IMRT; Gd:Gadolinium; PWI:perfusion weighted imaging ; ROI:regions of interest ;

Declarations

Funding

Key Research Program of Shandong (No. 2018GSF118006)

National Key Research and Development Program of China (2017YFC0113202)

Availability of data and materials

The datasets used and/or analyzed during the current study are available from the corresponding author on reasonable request.

Authors' contributions

YXWand GZG contributed to the study design, the patient enrollment, the data statistics and analysis and writing the manuscript.JL and YY contributed to reviewing the delineation. YS and LZW made important contributions in collecting the data and revising the content. All authors read and approved the final manuscript.

Ethics approval and consent to participate

Approval was obtained from the institutional research ethics board of the Shandong Tumor Hospital Ethics Committee.

Consent for publication

Not applicable.

Competing interests

The authors declare that they have no competing interests.

Author details

[1]Shandong Cancer Hospital and Institute, Shandong First Medical University and Shandong Academy of Medical Sciences，Jinan 250117, China

References

1. Jiang S, Eberhart CG, Lim M, Heo HY, Zhang Y, Blair L, Wen Z, Holdhoff M, Lin D, Huang P, Qin H, Quinones-Hinojosa A, Weingart JD, Barker PB, Pomper MG, Laterra J, van Zijl PCM, Blakeley JO, Zhou J. Identifying Recurrent Malignant Glioma after Treatment Using Amide Proton Transfer-Weighted MR Imaging: A Validation Study with Image-Guided Stereotactic Biopsy. Clin Cancer Res. 2019;25(2):552–61. doi:10.1158/1078-0432.CCR-18-1233.
2. Leiva-Salinas C, Muttikkal TJE, Flors L, Puig J, Wintermark M, Patrie JT, Rehm PK, Sheehan JP, Schiff D. FDG PET/MRI Coregistration Helps Predict Response to Gamma Knife Radiosurgery in Patients With Brain Metastases. AJR Am J Roentgenol. 2019;212(2):425–30. doi:10.2214/AJR.18.20006.
3. Kessler AT, Bhatt AA. Brain tumour post-treatment imaging and treatment-related complications. Insights Imaging. 2018;9(6):1057–75. doi:10.1007/s13244-018-0661-y.
4. Stadlbauer A, Nimsky C, Gruber S, Moser E, Hammen T, Engelhorn T, Buchfelder M, Ganslandt O. Changes in fiber integrity, diffusivity, and metabolism of the pyramidal tract adjacent to gliomas: a quantitative diffusion tensor fiber tracking and MR spectroscopic imaging study. AJNR Am J Neuroradiol. 2007;28(3):462–9.
5. Cha S, Knopp EA, Johnson G, Wetzel SG, Litt AW, Zagzag D. Intracranial mass lesions: dynamic contrast-enhanced susceptibility-weighted echo-planar perfusion MR imaging. Radiology. 2002;223(1):11–29. doi:10.1148/radiol.2231010594.
6. Zach L, Guez D, Last D, Daniels D, Grober Y, Nissim O, Hoffmann C, Nass D, Talianski A, Spiegelmann R, Tsarfaty G, Salomon S, Hadani M, Kanner A, Blumenthal DT, Bukstein F, Yalon M, Zauberman J, Roth J, Shoshan Y, Fridman E, Wygoda M, Limon D, Tzuk T, Cohen ZR, Mardor Y. Delayed contrast extravasation MRI: a new paradigm in neuro-oncology. Neuro Oncol. 2015;17(3):457–65. doi:10.1093/neuonc/nou230.

7. Grosu AL, Souvatzoglou M, Röper B, Dobritz M, Wiedenmann N, Jacob V, Wester HJ, Reischl G, Machulla HJ, Schwaiger M, Molls M, Piert M. Hypoxia imaging with FAZA-PET and theoretical considerations with regard to dose painting for individualization of radiotherapy in patients with head and neck cancer. Int J Radiat Oncol Biol Phys. 2007;69(2):541–51. doi:10.1016/j.ijrobp.2007.05.079.
8. Hazle JD, Jackson EF, Schomer DF, Leeds NE. Dynamic imaging of intracranial lesions using fast spin-echo imaging: differentiation of brain tumors and treatment effects. J Magn Reson Imaging. 1997;7(6):1084–93. doi:10.1002/jmri.1880070622.
9. Zach L, Guez D, Last D, Daniels D, Grober Y, Nissim O, Hoffmann C, Nass D, Talianski A, Spiegelmann R, Cohen ZR, Mardor Y. Delayed contrast extravasation MRI for depicting tumor and non-tumoral tissues in primary and metastatic brain tumors. PLoS One. 2012;7(12):e52008. doi:10.1371/journal.pone.0052008.
10. Weybright P, Sundgren PC, Maly P, Hassan DG, Nan B, Rohrer S, Junck L. Differentiation between brain tumor recurrence and radiation injury using MR spectroscopy. AJR Am J Roentgenol. 2005;185(6):1471–6. doi:10.2214/AJR.04.0933.
11. Zhang H, Ma L, Wang Q, Zheng X, Wu C, Xu BN. Role of magnetic resonance spectroscopy for the differentiation of recurrent glioma from radiation necrosis: a systematic review and meta-analysis. Eur J Radiol. 2014;83(12):2181–9. doi:10.1016/j.ejrad.2014.09.018.
12. Sun J, Cai L, Zhang K, Zhang A, Pu P, Yang W, Gao S. A pilot study on EGFR-targeted molecular imaging of PET/CT With 11C-PD153035 in human gliomas. Clin Nucl Med. 2014;39(1):e20–6. doi:10.1097/RLU.0b013e3182a23b73.
13. Litter RA, Barjat H, Hare JI, Jennerb M, Watsona Y, Cheunga S, Hollidaya K, Zhanga W, O'Connord J, Barryc ST, Purie S, Parkera GM f. John C. Evaluation of dynamic contrast-enhanced MRI biomarkers for stratified cancer medicine: How do permeability and perfusion vary between human tumours? Magn ResonImaging. 2018;46:98–105.
14. Wang YL, Liu MY, Wang Y, Xiao HF, Sun L, Zhang J, Ma L. Zhongguo Yi Xue Ke Xue Yuan Xue Bao. 2013;35(4):416–21. doi:10.3881/j.issn.1000-503X.2013.04.011.
15. Haris M, Gupta RK, Husain M, Srivastava C, Singh A, Singh Rathore RK, Saksena S, Behari S, Husain N, Mohan Pandey C, Nath Prasad K. Assessment of therapeutic response in brain tuberculomas using serial dynamic contrast-enhanced MRI. Clin Radiol. 2008;63(5):562–74. doi:10.1016/j.crad.2007.11.002.
16. Noguchi T, Yoshiura T, Hiwatashi A, Togao O, Yamashita K, Nagao E, Shono T, Mizoguchi M, Nagata S, Sasaki T, Suzuki SO, Iwaki T, Kobayashi K, Mihara F, Honda H. Perfusion imaging of brain tumors using arterial spin-labeling: correlation with histopathologic vascular density. AJNR Am J Neuroradiol. 2008;29(4):688–93. doi:10.3174/ajnr.A0903.
17. Walker MD, Strike TA, Sheline GE. An analysis of dose-effect relationship in the radiotherapy of malignant gliomas. Int J Radiat Oncol Biol Phys. 1979;5(10):1725–31. doi:10.1016/0360-3016(79)90553-4.

18. Regine WF, Patchell RA, Strottmann JM, Meigooni A, Sanders M, Young AB. Preliminary report of a phase I study of combined fractionated stereotactic radiosurgery and conventional external beam radiation therapy for unfavorable gliomas. Int J Radiat Oncol Biol Phys. 2000;48(2):421–6. doi:10.1016/s0360-3016(00)00688-x.

Figures

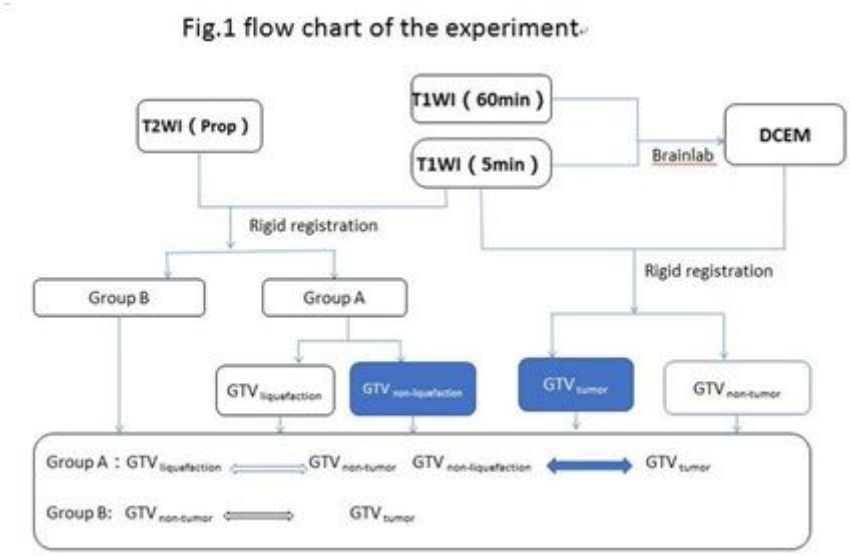

Figure 1

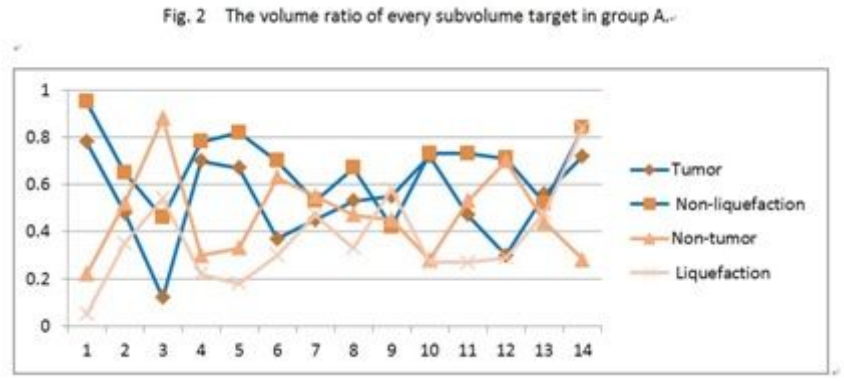

Figure 2

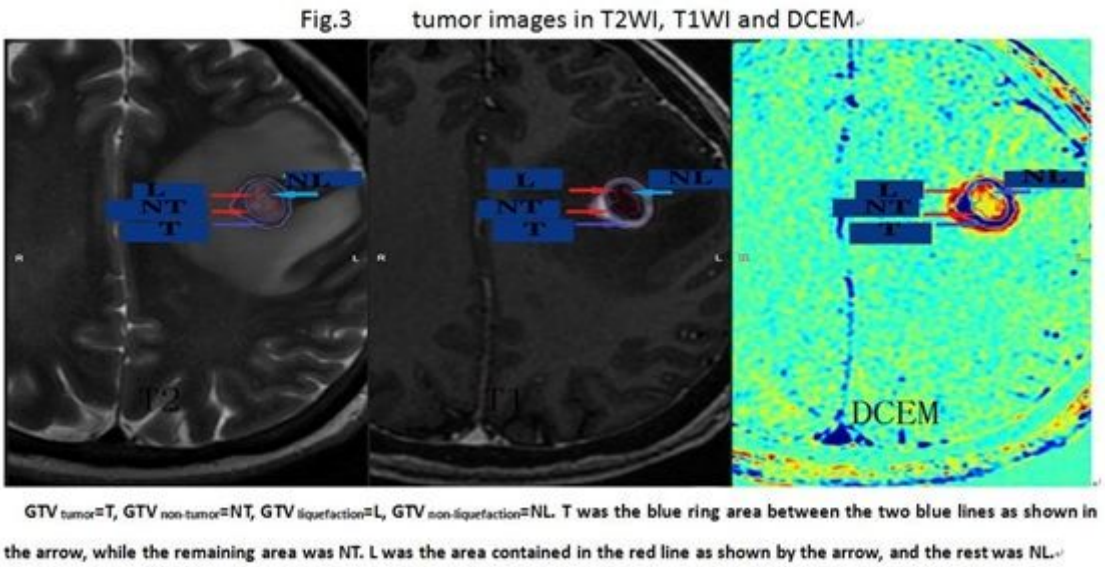

Figure 3

Supplementary Files

This is a list of supplementary files associated with this preprint. Click to download.

- Coverletter.docx
- Supportinformation.docx